1

3

4

5

6   Updated parameters and expanded simulation options for a model of the auditory

7   periphery

8

9   Muhammad S. A. Zilany[1]

10   Ian C. Bruce[2]

11   Laurel H. Carney[3]

12   [1]Department of Biomedical Engineering, Faculty of Engineering, University of Malaya,

13   Kuala Lumpur 50603

14   [2]Department of Electrical and Computer Engineering, McMaster University, Hamilton,

15   Canada, L8S 4K1

16   [3]Departments of Biomedical Engineering and Neurobiology & Anatomy, University of

17   Rochester, NY 14642

18

19

20   Running Title: An improved model of the auditory periphery

21

22   Date submitted: 6 November 2013

23

24 **ABSTRACT**

25 A phenomenological model of the auditory periphery in cats was previously developed

26 by Zilany and colleagues [J. Acoust. Soc. Am. **126**, 2390-2412 (2009)] to examine the

27 detailed transformation of acoustic signals into the auditory-nerve representation. In this

28 letter, a few issues arising from the responses of the previous version have been

29 addressed. The parameters of the synapse model have been readjusted to better simulate

30 reported physiological discharge rates at saturation for higher characteristic frequencies

31 [Liberman, J. Acoust. Soc. Am. **63**, 442-455 (1978)]. This modification also corrects the

32 responses of higher-CF model fibers to low-frequency tones that were erroneously much

33 higher than the responses of low-CF model fibers in the previous version. In addition, an

34 analytical method has been implemented to compute the mean discharge rate and

35 variance from the model's synapse output that takes into account the effects of absolute

36 refractoriness.

37

38

39

40

41

42

43 PACS numbers: 43.64.Bt, 43.64.Pg, 43.64.Wn [WPS]

44

45

46

47 **I. INTRODUCTION**

48   The auditory periphery is the sole conduit for acoustic information to reach the

49 higher auditory centers. Thus a detailed understanding of the transformation of acoustic

50 signals in the auditory periphery is necessary to determine how changes or deficits in

51 certain underlying mechanisms in the healthy or impaired ear may affect perception. A

52 phenomenological model of auditory-nerve responses in cats has been developed over the

53 years (Carney, 1993; Zhang *et al.*, 2001; Bruce *et al.*, 2003, Zilany and Bruce, 2006,

54 2007; Zilany *et al.*, 2009) to determine how the underlying sensory and neural

55 mechanisms affect neural representations, and more specifically to understand the staged

56 transformations at different levels of the auditory periphery. The most recently published

57 model (Zilany *et al.*, 2009), which will be subsequently referred to as the "2009 version",

58 incorporates most of the nonlinearities observed at the level of the AN, such as nonlinear

59 tuning, level-dependent phase, compression, suppression, shift in the best frequency as a

60 function of level, adaptation, as well as some other nonlinearities seen at high sound

61 levels. The 2009 version also includes power-law dynamics in the model of the inner-

62 hair-cell (IHC)-AN synapse, which substantially improves the prediction of AN

63 responses to a wide variety of complex sounds such as amplitude-modulated (AM)

64 stimuli, responses to forward-masking paradigms (Zilany *et al.*, 2009), and also the long-

65 term dynamics of AN responses (Zilany and Carney, 2010).

66   Although the 2009 version of the AN model captures features of responses in cat to

67 a wide variety of simple (tone-like) and complex (speech and noise) acoustic stimuli, the

68 model does not accurately simulate the data from Liberman (1978) describing the

69 discharge rate at saturation as a function of characteristic frequency (CF) for higher CFs.

70   The synapse model of the 2009 version has exponential adaptation followed by power-

71   law adaptation. The synapse parameters, particularly the steady-state (Ass) and the

72   spontaneous rate (Asp) of the three-store diffusion model (Westerman and Smith, 1988)

73   were adjusted and set as a function of CF when the power-law adaptation was added to

74   the model. Unfortunately, it has subsequently been realized that the model saturation

75   rates at higher frequencies to CF tones are significantly higher than the rates described by

76   Liberman (1978). Also, the responses of higher-CF model fibers to low-frequency tones

77   are erroneously much higher than the responses of low-CF model fibers to the same

78   stimuli. This problem is evident from the response area to a 500-Hz tone signal (Fig. 1A).

79   To address the problem mentioned above, some parameters of the IHC-AN

80   synapse section of the model have been modified to limit the saturation rate of fibers as a

81   function of CF to be more consistent with the data reported in Liberman (1978). Also, an

82   analytical method has been adopted to compute the mean and variance of the discharge

83   rate as a function of time from the model synapse output (before the discharge generator),

84   accounting for the refractory effects of the AN. A new version of the model incorporating

85   all of the above-mentioned changes is available on the following website

86   (http://www.urmc.rochester.edu/labs/Carney-Lab/publications).

87

88   II. MODIFICATIONS OF THE MODEL AND RESULTS

89   A. Saturation rate as a function of CF

90   In the IHC-AN synapse section of the model (Zilany *et al.*, 2009), a three-store

91   diffusion model is followed by a power-law adaptation. Westerman and Smith's (1988)

92   three-store diffusion model produces an exponential adaptation with rapid and short-term

4

93   time constants, and the output of this exponential adaptation stage is further adapted by

94   the power-law dynamics. The power-law model has also two paths, namely slow and fast.

95   In general, the power-law affects (adapts) constant (dc) signals, which arise for the higher

96   CFs because of the low-pass filter in the IHC, more than the respective fluctuating signals

97   (which arise for the lower CFs). Therefore, in the Zilany *et al.* (2009) model, the steady-

98   state rate (*Ass*) parameter of the double-exponential adaptation was adjusted as a function

99   of CF to achieve the desired responses to CF tones. However, this change resulted in

100   higher saturation discharge rates (to CF tones) for model fibers with CFs above ~2 kHz

101   than reported in Liberman (1978). In addition, this adjustment created a problem of much

102   higher saturation rates of model high-CF fibers to low-frequency tones than the saturation

103   responses of low-frequency fibers to the same low-frequency stimulus. Simply

104   readjusting the parameter *Ass* as a function of CF can solve the former problem, *i.e.*, the

105   model saturation rate can be made to match AN data for high-CF fibers. However, the

106   latter problem still persists; the response area plot in Fig. 1A shows that the rates of high-

107   CF fibers in response to a low frequency tone (500 Hz) were much higher than the

108   responses of low-CF fibers to the same tone. To solve this problem, it was necessary to

109   readjust the parameters of the power-law model to achieve responses that agree with the

110   cat AN data.

111   A general model of power-law adaptation (Drew and Abbott, 2006) is described as

112   follows. Suppose, a stimulus *s(t)* produces a response *r(t)* that feeds back into an

113   integrator *I(t)*, such that the adapted response is described as, $r(t) = \max[0, s(t)-I(t)]$. The

114   suppressive effects are accumulated with power-law memory, and are given by the

115   following equation.

$$I(t) = \alpha \int_0^t \frac{r(t')}{t-t'+\beta} dt' = \alpha\, r(t) * f(t), \text{ where } f(t) = 1/(t + \beta). \tag{1}$$

116   Here α is a dimensionless constant that controls the amount of adaptation, β is a

117   parameter with units of time, and ∗ indicates convolution (Drew and Abbott, 2006).

118   In this work, the amount of adaptation applied to higher CFs has been readjusted by

119   changing the parameter α in the slow power-law path. With the combination of changing

120   α from 5×10^{-6} to 2.5×10^{-6} and readjustment of *Ass* as a function of CF [*Ass* = 800×

121   (1+CF/10^5) where CF is in units of Hz], the desired responses of the model have been

122   achieved. The responses of the new model are shown in Fig. 1B, along with the responses

123   from the 2009 version of the model. The model saturation rate as a function of

124   characteristic frequency is compared with the physiological data from cats (Liberman,

125   1978) in Fig. 2. The acoustic stimuli used were 50-ms tone bursts with a 2.5 ms rise-fall

126   time, and the rate of stimulus presentation was 10/s. Following the same paradigm, model

127   rate-level responses were simulated for a range of CFs for sound levels ranging from 0 to

128   100 dB SPL, and the discharge rate at saturation was estimated for each CF. Although the

129   proposed model responses (shown by asterisks) are within a reasonable range of the

130   published physiological data (circles), the discrepancy at lower CFs could lie in the fact

131   that the saturation rate for the physiological data (Liberman, 1978) was computed from

132   the rate-level responses for sound levels up to and including 54 dB above threshold.

133   However, the model responses have been simulated at even higher levels to be able to

134   estimate a measurable saturation rate. The new model has also been extensively tested

135   against the published and recorded data from the AN, and the results are summarized in

136   Table I. As expected, only the responses to forward-masking paradigm are affected by

137   this change, although minimally; other responses are apparently unchanged.

138   In the 2009 version of the model, a fractional Gaussian noise (fGn) was added in

139   the slow power-law path in order to model the distribution of spontaneous rates reported

140   in Liberman (1978). A fractional (fractal) Gaussian noise is a generalization of the

141   common white Gaussian noise that shows long range dependence. In this work, the

142   option to use a pre-determined fixed seed instead of a variable seed for the fGn is made

143   available; using the fixed seed removes the trial-to-trial variability in this aspect of the

144   model response, which is useful to separate the independent effects of internal

145   (physiological) and external (stimulus) noise. The fixed seed chosen in the code gives a

146   fairly average synapse response.

147   B. Analytical method to estimate mean rate and variance from the synapse output

148   The output of the model IHC section drives the IHC-AN synapse model, which

149   provides an instantaneous synaptic release rate as output without taking into account the

150   refractory effects (absolute and relative). In the final stage of the model, the discharge

151   times are produced by a renewal process that includes refractory effects. However, to

152   obtain a reliable post-stimulus time histogram (PSTH) based on the output of the

153   discharge generator requires simulating responses to multiple repetitions of the same

154   stimulus. To make the model computationally efficient, it is useful to employ a synapse

155   output for which the effects of refractoriness can be directly estimated. Thus an analytical

156   methodology has been applied here to calculate an approximate mean rate and variance

157   as a function of time, including refractory effects, from the model synapse output.

158   Vannucci and Teich (1978) derived a general expression for the dead-time

159   (absolute refractory period) modified mean and variance for a counting process when the

160   rate of input is an arbitrary function of time. Edwards and Wakefield (1990) also derived

161 an analytical solution to compute the mean rate of nerve firing as a function of time (eq.

162 21 and 22 in Edwards and Wakefield, 1990), considering both the absolute and relative

163 refractory effects. The latter method requires recursion and is computationally very

164 expensive. However, the former method does not include relative refractory effects. In

165 both cases, the assumption is that the rate of the input process is nearly constant with

166 respect to the duration of the absolute refractory period. In the revised model presented

167 here, the mean rate was computed from the model synapse output using the same

168 recovery function as used in the discharge generator section of the 2009 version of the

169 model (Zilany *et al.*, 2009). The estimated rates are almost the same for both methods

170 (Vannucci and Teich, 1978; Edwards and Wakefield, 1990) when the synapse output is

171 fairly constant. Note that the estimate of mean rate deviates from the model PSTH when

172 the synapse output changes rapidly, because it violates the basic assumption made in both

173 cases. This has been illustrated in Fig. 3. When the synapse output (solid line) is nearly

174 constant or varies slowly, the estimated mean rate (dashed line, using Vannucci and

175 Teich, 1978) closely matches the model PSTH (dotted line) from the output of the

176 discharge generator (Fig. 3A). However, when the synapse output varies abruptly,

177 especially at the onset of the responses at higher levels (Fig. 3B), the estimated mean rate

178 is substantially higher than the rate computed from the PSTH of the model AN discharge

179 generator. However, the estimated mean rate still provides a better prediction of the

180 PSTH than does the synapse output.

181   To make the calculation computationally less expensive, the following expression

182 by Vannucci and Teich (1978) has been implemented in the code:

$$R(t) = \frac{Sout(t)}{1 + \tau Sout(t)}, \tag{2}$$

183 where $R(t)$ is the mean discharge rate as a function of time, $Sout(t)$ is the model synapse

184 output (spikes/sec), and τ is the absolute refractory period (here fixed to 0.75 ms). The

185 variance of the rate can be computed as [eq. 12 in Vannucci and Teich, 1978]:

$$\sigma^2(t) = \frac{Sout(t)}{[1 + \tau Sout(t)]^3} \, . \tag{3}$$

186

187 **III. CONCLUSIONS**

188   A revised phenomenological model of the auditory periphery is presented here. The

189 changes made to the 2009 version corrected the model saturation rates as a function of

190 CF without adversely affecting other response properties. The forward-masking

191 properties were affected to a small degree, as could be expected after modifying synaptic

192 adaptation. The effects of refractoriness have been incorporated into the model of the

193 IHC-AN synapse. The model is now a better candidate to examine realistic neural-

194 encoding hypotheses, especially those involving high CFs.

195

202

203 **REFERENCES**

204   Bruce, I. C., Sachs, M. B., and Young, E. D. (**2003**). "An auditory-periphery model of the

205   effects of acoustic trauma on auditory nerve responses," J. Acoust. Soc. Am. **113**, 369–

206   388.

207   Carney, L. H. (**1993**). "A model for the responses of low-frequency auditory-nerve fibers

208   in cat" J. Acoust. Soc. Am. **93**(1), 401-417.

209   Drew, P. J., and Abbott, L. F. (**2006**). "Models and properties of power-law adaptation in

210   neural system," J. Physiol. **96**, 826–833.

211   Edwards, B. W., and Wakefield, G. H. (**1990**). "On the statistics of binned neural point

212   processes: the Bernoulli approximation and AR representation of the PST histogram,"

213   Biol. Cybern. **64**, 145–153.

214   Joris, P. X., and Yin, T. C. T. (**1992**). "Responses to amplitude-modulated tones in the

215   auditory nerve of the cat," J. Acoust. Soc. Am. **91**, 215–232.

216   Liberman, M. C. (**1978**). "Auditory-nerve response from cats raised in a low-noise

217   chamber," J. Acoust. Soc. Am. **63**(2), 442–455.

218   Louage, D. H. G., Heijden, M. v. d., and Joris, P. X. (2004). "Temporal properties of

219   responses to broadband noise in the auditory nerve," J. Neurophysiol. **91**, 2051–2065.

220   Smith, R. L., Brachman, M. L., and Frisina, R. D. (1985). "Sensitivity of auditory-nerve

221   fibers to changes in intensity: A dichotomy between decrements and increments," J.

222   Acoust. Soc. Am. **78**(4), 1310–1316.

223   Vannucci, G., and Teich, M. C. (**1978**). "Effects of rate variation on the counting

224   statistics of dead-time-modified Poisson processes," Optics Communications **25**(2), 267–

225   272.

226 Westerman, L. A., and Smith, R. L. (**1988**). "A diffusion model of the transient response

227 of the cochlear inner hair cell synapse," J. Acoust. Soc. Am. **83**(6), 2266–2276.

228 Young, E. D., and Sachs, M. B. (1973). "Recovery from sound exposure in auditory-

229 nerve fibers," J. Acoust. Soc. Am. **54**(6), 1535–1543.

230 Zhang, X., Heinz, M. G., Bruce, I. C., and Carney, L. H. (**2001**). "A phenomenological

231 model for the responses of auditory-nerve fibers. I. Nonlinear tuning with compression

232 and suppression," J. Acoust. Soc. Am. **109**, 648–670.

233 Zilany, M. S. A., and Bruce, I. C. (**2006**). "Modeling auditory-nerve responses for high

234 sound pressure levels in the normal and impaired auditory periphery," J. Acoust. Soc.

235 Am. **120**, 1446–1466.

236 Zilany, M. S. A., and Bruce, I. C. (**2007**). "Representation of the vowel /ɛ/ in normal and

237 impaired auditory nerve fibers: Model predictions of responses in cats," J. Acoust. Soc.

238 Am. **122**(1), 402–417.

239 Zilany, M. S. A., Bruce, I. C., Nelson, P. C., and Carney, L. H. (**2009**) "A phenomeno-

240 logical model of the synapse between the inner hair cell and auditory nerve: long-term

241 adaptation with power-law dynamics," J. Acoust. Soc. Am. **126,** 2390–2412.

242 Zilany, M. S. A., and Carney, L. H. (**2010**) "Power-law dynamics in an auditory-nerve

243 model can account for neural adaptation to sound-level statistics," J. Neurosci. **30**(31),

244 10380-10390.

245

246

247

248

249   **TABLE**

250

251   Table 1: Lists of model response properties that remained almost unchanged from the

252   2009 version after the modifications proposed in this paper.

253

No	Response property
1	Distribution of spontaneous rates (Liberman, 1978)
2	Long-term recovery (Young and Sachs, 1973)
3	Responses to stimuli with amplitude increments/decrements (Smith et al., 1985)
4	Responses to SAM tones (Joris and Yin, 1992)
5	Responses to noise stimuli (Louage et al., 2004)

FIGURE CAPTIONS

FIG 1. Responses of a population of AN model fibers to a 500-Hz tone (50-ms duration with 2.5 ms on/off ramp) presented across a range of sound levels. Mean rate responses are shown for 100 AN fibers with CFs logarithmically spaced from 200 Hz to 20 kHz (along the x-axis) and sound levels ranging from -15 to 120 dB SPL (along the y-axis) in steps of 2.5 dB. A) Responses from the Zilany *et al.* (2009). B) Responses from the model presented here.

FIG 2. Discharge rate at saturation as a function CF for HSR fibers. Physiological saturation rates (reprinted Fig. 17 from Liberman, 1978 with permission), shown by circles, were determined at each CF from the AN rate-level responses for sound levels up to and including 54 dB above threshold. Model saturation rate (shown by asterisks) at each CF was estimated from the simulated rate-level responses using the paradigm in Liberman (1978), except that the sound levels were extended up to 100 dB SPL to obtain a measurable saturation rate.

FIG 3. Illustrations of the effect of changes in the stimulus on the model synapse output and discharge generator. The response of a tone at CF is shown for a model HSR fiber with CF equal to 10 kHz. The duration of the stimulus was 100 ms with a rise time of 50 ms (slowly-varying). PSTH responses were simulated for 100 repetitions of the same stimulus, and the repetition time was 120 ms. A: Responses at near threshold (8 dB SPL). B: Responses at 40 dB SPL. The estimate of mean rate (dashed line) deviates from the PSTH output (dotted line) when the synapse output (solid line) varies abruptly, especially at the onset of the model AN responses to higher level tones.
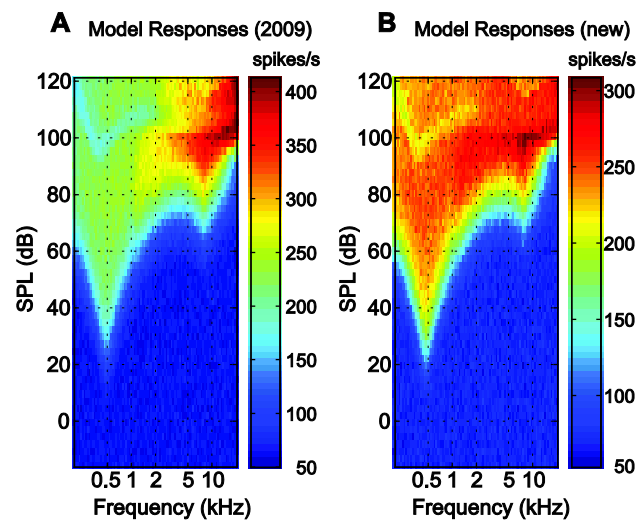
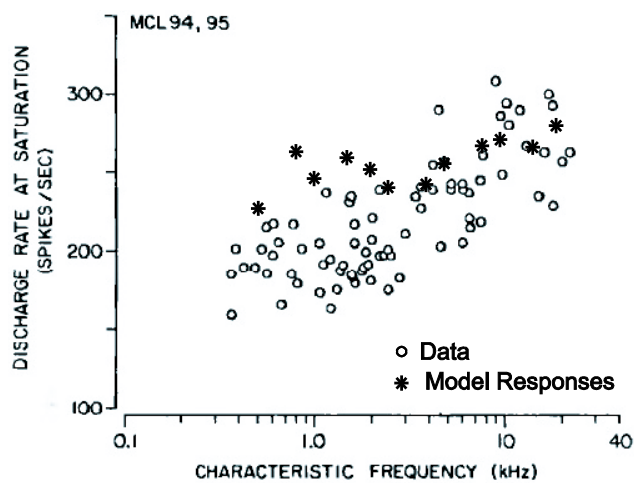**A** Model Responses (2009)
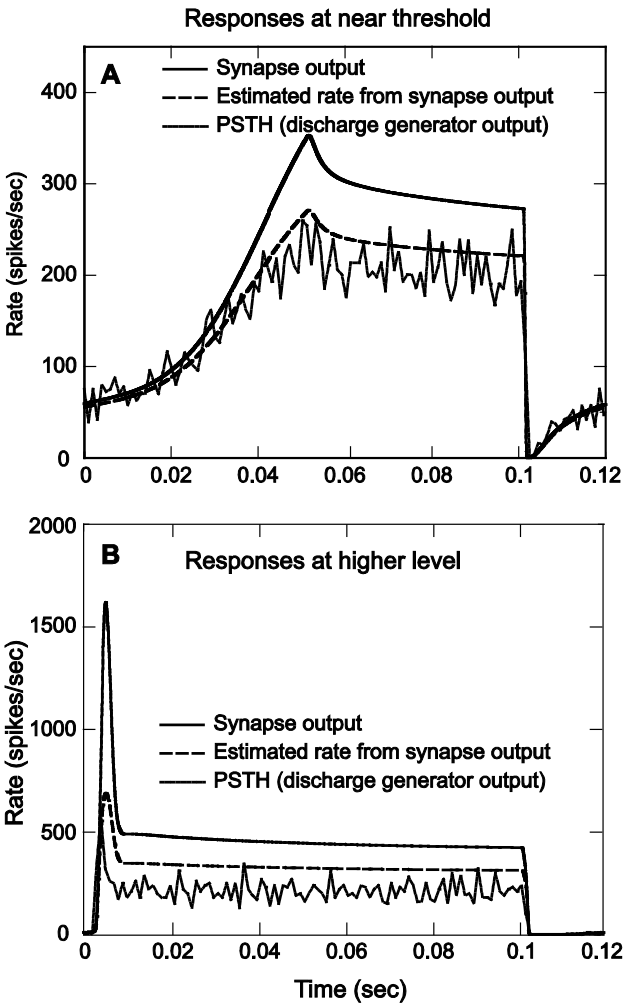
B Model Responses (new)

FIGURE 1

FIGURE 2

FIGURE 3